

See discussions, stats, and author profiles for this publication at: <https://www.researchgate.net/publication/45279237>

# Looped back fiber mode for reduction of false alarm in leak detection using distributed optical fiber sensor

Article in *Applied Optics* · July 2010

DOI: 10.1364/AO.49.003869 · Source: PubMed

CITATIONS

12

READS

242

7 authors, including:



**Pandian Chelliah**

Ramakrishna Mission Vivekananda College, India

32 PUBLICATIONS 110 CITATIONS

[SEE PROFILE](#)



**Sosamma Samvel**

Indira Gandhi Centre for Atomic Research

25 PUBLICATIONS 83 CITATIONS

[SEE PROFILE](#)



**Babu Rao Dr C**

Indira Gandhi Centre for Atomic Research

102 PUBLICATIONS 554 CITATIONS

[SEE PROFILE](#)



**Murali Nagarajan**

Indira Gandhi Centre for Atomic Research

2 PUBLICATIONS 12 CITATIONS

[SEE PROFILE](#)

Some of the authors of this publication are also working on these related projects:



Thermography [View project](#)



Metal Matrix Nanocomposites [View project](#)

# Looped back fiber mode for reduction of false alarm in leak detection using distributed optical fiber sensor

Pandian Chelliah, Kasinathan Murgesan, Sosamma Samvel, Babu Rao Chelamchala,\*  
Jayakumar Tammana, Murali Nagarajan, and Baldev Raj

Indira Gandhi Centre for Atomic Research, Kalpakkam, India 603102

\*Corresponding author: cbr@igcar.gov.in

Received 16 February 2010; revised 5 June 2010; accepted 14 June 2010;  
posted 15 June 2010 (Doc. ID 124246); published 5 July 2010

Optical-fiber-based sensors have inherent advantages, such as immunity to electromagnetic interference, compared to the conventional sensors. Distributed optical fiber sensor (DOFS) systems, such as Raman and Brillouin distributed temperature sensors are used for leak detection. The inherent noise of fiber-based systems leads to occasional false alarms. In this paper, a methodology is proposed to overcome this. This uses a looped back fiber mode in DOFS and voting logic is employed to considerably reduce the false alarm rate. © 2010 Optical Society of America  
OCIS codes: 060.2370, 120.6780, 290.5860.

## 1. Introduction

Optical-fiber-based sensors with inherent advantages, such as immunity to electromagnetic interference, flexibility, low material reactivity, and long transmission distances [1–3], provide more desirable solutions for leak monitoring compared to the alternatives, such as pressure monitoring using flow meters, spark-plug-based and mutual inductance, primary coolant inventory balance, acoustic-monitoring-based leak detectors, or Doppler-frequency-shift-based ground-penetrating radar [4–6].

MacLean *et al.* [7] used the principle of microbending-induced loss in optical fibers for detection of hydrogen leakage. Huang *et al.* [8] used a hybrid configuration that included Mach–Zehnder and Sagnac interferometers for detection (detection of acoustic signal generated by leak). Qu *et al.* used a Mach–Zehnder-based distributed fiber optic sensor for leak detection [9]. Leak detection in oil/gas pipelines using a Raman distributed temperature sensor (RDTS) has been studied by monitoring the temperature change associated with leaks [10]. Temperature increases in the case of an oil leak and the tempera-

ture drops when there is a gas leak. Jensen *et al.* [11] used RDTS for leak detection for coolant leakage in the JOYO reactor, and Nikles *et al.* [12,13] demonstrated leak detection using a Brillouin-based distributed sensor on pipelines. Inaudi *et al.* [14] discussed the parameters that affect the response time and detection volume, such as the relative position of the leak to the sensing cable and the temperature contrast between the fiber and the ambience where it is embedded for a distributed fiber optic temperature sensor systems based on Raman and Brillouin scattering. They also presented results of oil microleakage and gas leakage simulation results. A good discussion on leak detection using a distributed fiber optic sensor can be found in [15].

Reduction of false alarms in sensor systems is a very important problem in the areas where the sensors can be applied. Optical-fiber-based sensors are no exception.

The temperature measurement in fiber-based systems, such as Raman and Brillouin distributed sensors, are statistical in nature and thus have inherent noise. This noise leads to error and consequently to occasional false alarms in leak detection. Zhang [16] discussed seven attributes that are necessary for a good leak detection system. Important among them are leak sensitivity and false alarm rate.

A signal-processing-based method to reduce false alarm in a Sagnac-interferometer-based sensor has been demonstrated [17]. However, the reduction in false alarms is based on pattern recognition (discerning different signals) and is implemented at the signal processing (*postprocessing*) step. The error in optical-fiber-based RDTSs is not completely understood. To the best of our knowledge, there is no literature available that discusses the false alarm rate for fiber-optic-sensor-based leak detection systems.

## 2. Problem Description

In general, the total error in the measurement can be classified into three types.

i. Spatial errors  $\epsilon_{\text{spatial}}$ . These errors correspond to the presence of microbends, macrobends, cracks, and residual stress impressed on the fiber. These errors can be reduced by employing a calibration/correction procedure [18].

ii. Temperature-dependent errors  $\epsilon_{\text{temp}}$ . The response of the optoelectronic hardware is a function of the temperature. To take care of this, an RDTS is provided with a set of platinum-based resistance temperature devices (RTDs). The RTDs are kept in a constant temperature bath. The RDTS dynamically calibrates the temperature with that measured by the RTDs. Any temperature-dependent noise in the RDTS is thus minimized.

iii. Statistical errors  $\epsilon_{\text{statistical}}$ . The statistical errors are the source of false alarms. A specific random temporal noise in the RDTS corresponds to noise in a specific spatial location, leading to a false alarm. It is well known that the statistical noise can be reduced by increasing the measurement time. However, a longer measurement time in a leak detection system defeats the system's own purpose, which is detecting a leak at the earliest possible moment for early warning.

Thus,

$$T_{\text{meas}} = T + \epsilon_{\text{spatial}} + \epsilon_{\text{temp}} + \epsilon_{\text{statistical}}, \quad (1)$$

where  $T$  is the actual temperature of the zone being measured.

The method of applying threshold has been used before [19] for an RDTS-based sensor. A threshold is defined based on long-term study of the noise in nonleak environments. A leak is said to occur if the temperature rises above this threshold.

An RDTS measures integral temperature over one pulse width of the laser. This length corresponds to spatial resolution, and is of the order of 1 m. The leak, however, occurs over a length of a few centimeters. Because of this integral nature of temperature measurement, a temperature rise of 80 °C registers as only a 2° or 3° rise in the RDTS measurement [19]. This is especially true in cases of small leaks where the temperature rise is minimal. In such cases, there are two distinct possibilities. When there

is a leak and  $T_{\text{meas}} < \text{Threshold}$ , this corresponds to no alarm. This is not a serious issue. With an accumulation of leaks, an alarm would eventually be raised. With an accumulation of leaks, an alarm would eventually be raised. When there is no leak and  $T_{\text{meas}} > \text{Threshold}$ , this corresponds to a false alarm. Such a false alarm requires visual verification for corrective action. This often leads to stoppage of work. For small leaks, if we keep a high threshold to reduce false alarms, the leak may not be detected. For a lower threshold, the leak will be detected, but the number of false alarms will increase.

In this paper, therefore, we address the issue of false alarms, and demonstrate a methodology to reduce the same.

When a physical field is measured using a sensor, there is always a possibility of false alarms from different sources of error. The general practice is to use redundant sensors. Measurements in critical applications, such as reactors and satellites, require high reliability and low false alarm rate. An appropriate voting logic [20,21] is employed along with redundancy to increase the reliability and reduce false alarms. However, if a single system with multiple sensors is used, the burden of time on multiplexing is large. It is also possible to use multiple sensors with multiple systems for parallel measurement. But this would require the actual deployment of multiple systems. In our case, the looped back fiber mode provides the redundant measurement without the need for multiplexing or multiple systems. The RDTS measures the temperature along the entire length of the fiber in a single measurement. The voting logic is used to reduce false alarms. The looped back configuration has earlier been used by Höbel *et al.* [22] and di Vita and Rossi [23] to correct for attenuation in a distributed sensor for temperature measurement. In the looped back system, the mode temperature of a single zone is measured twice by two sections of fiber. We have used this redundancy in a looped back fiber mode to implement a 2 × 2 voting logic to reduce false alarms in leak detection using an RDTS.

## 3. Experimental Setup

### A. Raman Distributed Temperature Sensor System

An RDTS combines the principle of optical time domain reflectometer and the temperature dependence of Raman scattering. This makes distributed temperature measurement along the entire length of the fiber possible. The schematic of the working of an RDTS is presented in Fig. 1.

A laser pulse is launched into the fiber. It gets scattered at every point in the fiber. The backscattered Stokes and anti-Stokes–Raman lines are separated using filters. The ratio of the intensity is measured, and is converted into temperature. A more detailed description of an RDTS can be found in [10,24].

The RDTS used in this experiment is a Sensornet RDTS, which uses a Nd:YAG laser operating at 1.06 nm, with a pulse width of 5 ns. The system has

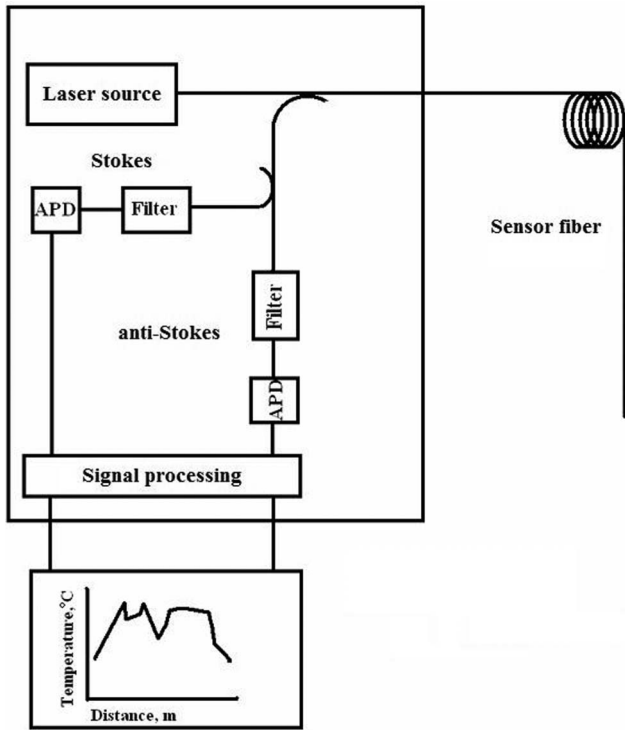


Fig. 1. Schematic of RDTS system.

a minimum measurement time of 10 s, and its highest spatial resolution is 1 m.

#### B. Leak Setup

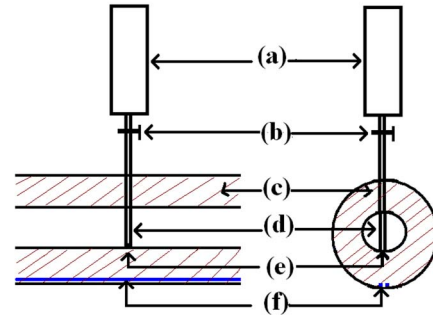
An experimental leak setup consisting of a pipeline and a simulated leak source was erected in the laboratory (Figs. 2A and 2B). The length of the loop is 2 m and the height is 1 m. Water is used as the leaking medium. The leak source consists of a funnel. The bottom of the funnel is provided with a valve and an outlet tube of 5 mm internal diameter. The outlet tube enters the pipe (at the 12 o'clock position), is placed along the diameter of the pipe perpendicular to its axis, and exits at the bottom of the pipe (at the 6 o'clock position). The end of the tube is flushed with the bottom surface of the pipe and is provided with a fissure of 3 mm diameter. The leak rate can be controlled from 1 to 10 ml/s by controlled opening of the valve. The funnel is provided with a separate heater. With this arrangement, it is possible to have independent control of the loop's temperature and the temperature of the leaking water. A thermocouple is placed in the funnel to monitor the temperature of the leaking medium. A thermocouple is also placed along with the fiber for comparing with the RDTS measurements.

#### C. Fiber Laying Methodology

When a leak occurs, the leaking medium percolates down through the insulating material. If a fiber is laid immediately below the pipe, some of the leak may not be detected. If the fiber is laid far below the pipe, the percolating leaking medium loses heat in the process, and the contrast in the heat between the leaking



A



B

Fig. 2. (Color online) A, test loop to test optical-fiber-based distributed sensor for temperature sensor. B, leak setup: (a) funnel, (b) valve, (c) insulation, (d) feed tube, (e) fissure, (f) fiber.

medium and the fiber becomes minimal. The fiber position is optimized according to the temperature of the leaking medium and that of the insulation (ambience). The fiber is laid at the 6 o'clock position, below the insulation and above the metal cladding, in a looped back mode. A schematic of the fiber position is shown in Fig. 3.

#### 4. Discussion on Error

Consider a fiber laid singly on the loop probed using the RDTS [Fig. 3(a)]. Fiber section  $AD$  corresponds to the length of the pipe and is continuously monitored. The leak source is located in section  $L$  of the loop. The

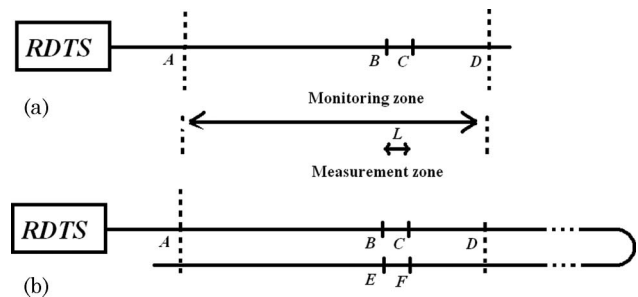


Fig. 3. (a) Fiber is laid singly. The entire fiber section  $AD$  is monitored. The leak at measurement zone  $L$  is measured by fiber section  $BC$ . (b) Fiber is laid in looped back mode. The entire fiber section  $AD$  is monitored. The leak at measurement zone  $L$  is measured by fiber section  $EF$ , in addition to section  $BC$ .

fiber section  $BC$  measures the temperature of section  $L$ . This measurement zone is 1 m in length, because of the spatial resolution limit.

The temperature,  $T$ , measured at  $L$  by fiber section  $BC$  [using Eq. (1)] is given by

$$T_{\text{meas}}(BC) = T(BC) + \varepsilon_{\text{spatial}}(BC) + \varepsilon_{\text{temp}}(BC + \varepsilon_{\text{statistical}}(BC)). \quad (2)$$

At ambient temperature, the fiber sections are monitored for time  $\tau$ . The mean temperature for the temperature measured during this interval is  $T_{\text{mean}}$  and the standard deviation is  $\sigma$ .

The threshold for leakage is defined as

$$T_{\text{thresh}} = T_{\text{mean}} + n_{\text{thresh}}\sigma, \quad (3)$$

where  $n_{\text{thresh}}$  is a positive rational. The threshold  $= n_{\text{thresh}}\sigma$  must be optimized. That is, if the temperature measured is more than  $T_{\text{thresh}}$ , a leak is said to have occurred.

The probability that a false alarm occurs is given by

$$P(|T - T_{\text{mean}}| > n_{\text{thresh}}\sigma) = \sqrt{\frac{2}{\pi}} \int_{n_{\text{thresh}}}^{\infty} e^{-y^2/2} dy = \text{erfcf} \frac{n_{\text{thresh}}}{2},$$

where

$$y = \frac{T - T_{\text{mean}}}{\sigma \sqrt{2}}.$$

If  $n_{\text{thresh}} = 1$ ,

$$P(|T - T_{\text{mean}}| > \sigma) = 0.3173.$$

If  $n_{\text{thresh}} = 2$ ,

$$P(|T - T_{\text{mean}}| > 2\sigma) = 0.0455.$$

If  $n_{\text{thresh}} = 3$ ,

$$P(|T - T_{\text{mean}}| > 3\sigma) = 0.0027.$$

In looped back mode [Fig. 3(b)], the temperature is measured at the segment  $EF$ , in addition to  $BC$ , and is given, as in Eq. (4), by

$$T_{\text{meas}}(EF) = T(EF) + \varepsilon_{\text{spatial}}(EF) + \varepsilon_{\text{temp}}(EF) + \varepsilon_{\text{statistical}}(EF), \quad (4)$$

and the probability is given by

$$P(|T - T'_{\text{mean}}| > n_{\text{thresh}}\sigma') = \sqrt{\frac{2}{\pi}} \int_{n_{\text{thresh}}}^{\infty} e^{-y^2/2} dy = \text{erfcf} \frac{n_{\text{thresh}}}{2},$$

where

$$y = \frac{T - T'_{\text{mean}}}{\sigma' \sqrt{2}}.$$

For a  $2 \times 2$  voting logic, with the fiber laid in looped back mode, a leak is said to occur only when both measurement zones  $BC$  and  $EF$  indicate leakage. The temperatures measured at these two zones are independent of each other. The probability of a false alarm is given by

$$P = P(|T - T_{\text{mean}}| > n\sigma) * P(|T - T'_{\text{mean}}| > n\sigma').$$

If  $n_{\text{thresh}} = 1$ ,

$$P = P(|T - T_{\text{mean}}| > \sigma) * P(|T - T'_{\text{mean}}| > \sigma') = 0.1007.$$

If  $n_{\text{thresh}} = 2$ ,

$$P = P(|T - T_{\text{mean}}| > 2\sigma) * P(|T - T'_{\text{mean}}| > 2\sigma') = 0.0021.$$

If  $n_{\text{thresh}} = 3$ ,

$$P = P(|T - T_{\text{mean}}| > 3\sigma) * P(|T - T'_{\text{mean}}| > 3\sigma') = 7.2 \times 10^{-6}.$$

Thus it can be seen that the looped back mode of fiber laying reduces the probability of false alarms.

## 5. False Alarm Rate

In this experiment, the length of the loop is 6 m, shown by  $AB$  in Fig. 3(a). In the looped back fiber mode, twice this length falls on the loop. One meter of lead fiber on each fiber and 1 m of fiber

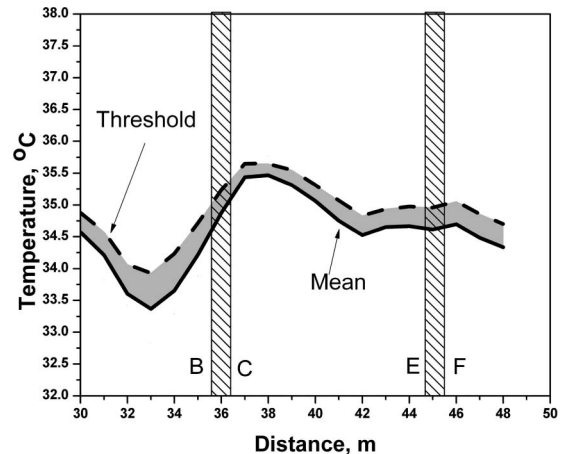


Fig. 4. Solid curve indicates the averaged measured temperature over the looped back fiber. The dashed curve indicates threshold equal to  $1\sigma$  above this averaged temperature.  $BC$  and  $EF$  are the measurement zones.

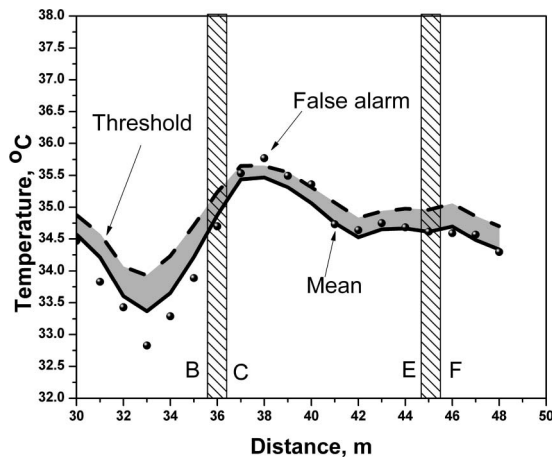


Fig. 5. Instance of a false alarm in a typical room temperature measurement. The solid circles represent instantaneous temperature measurements.

corresponding to the loop between the two is also monitored. Totally, a fiber length of 15 m is monitored. A given fiber monitors an 8 m zone (6 m loop + lead fiber) of this length. With a spatial resolution of 1 m, this length is divided into eight measurement zones.

Before the start of the leak, these eight measurement zones are monitored for 3 h using two fibers. When the measurement time of the system using an RDTS is 10 s, this measurement yields 8640 events for each sensor fiber. The mean ( $T_{\text{mean}}$ ) and standard deviation ( $\sigma$ ) over each zone of the fiber are determined. The average temperature measured in each zone is shown in Fig. 4. The undulations seen over the length of the fiber are due to  $\epsilon_{\text{fiber}}$ . The error bar over and above this average temperature is due to random error  $\epsilon_{\text{random}}$ . To detect a leak, a threshold is defined for each zone independently. Any temperature measurement above this threshold is deemed as a leak. The threshold thus defined is shown in Fig. 4.

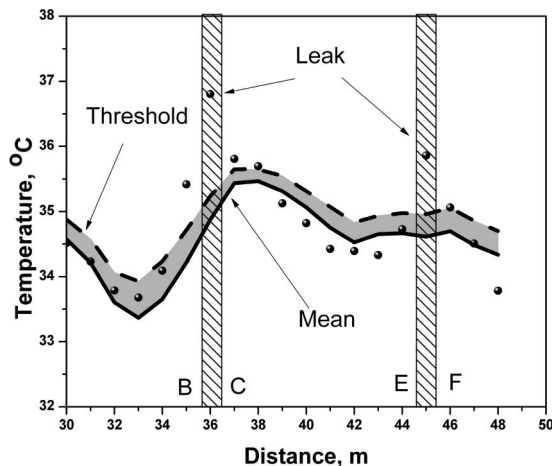


Fig. 6. Instance of leak detection in a typical temperature measurement in a leak. The solid circles represent instantaneous temperature measurements.

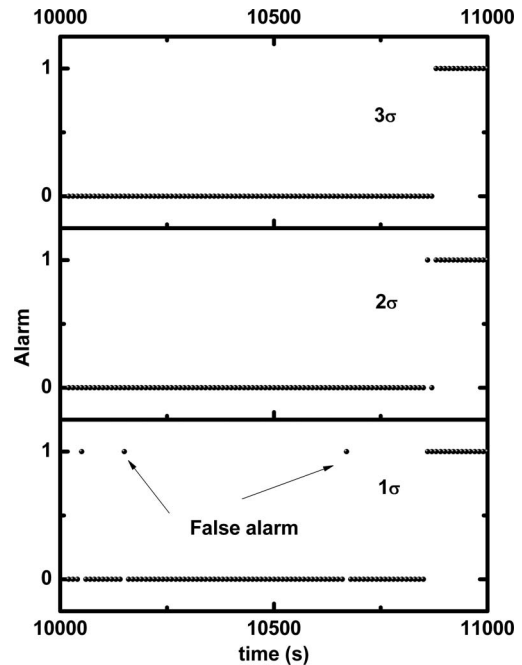


Fig. 7. Leak detection using the looped back fiber mode. Alarm = 1 indicates a leak.

The mean and the standard deviation are dynamically updated, to continuously define a new  $T_{\text{thresh}}$ . The data corresponding to a leak is not included for updating.

An instantaneous temperature measurement by fiber laid in the looped back mode indicating a typical false alarm is shown in Fig. 5. The temperature measurement at *BC* shows an erroneous rise above the allowed threshold. However, the temperature measured by section *EF* does not cross the threshold.

An instantaneous temperature measurement by the fiber laid in the looped back mode indicating a typical leak is shown in Fig. 6. The temperature rises both at *BC* and *EF*, indicating a leak. It may be observed that the temperature rise is observed not only

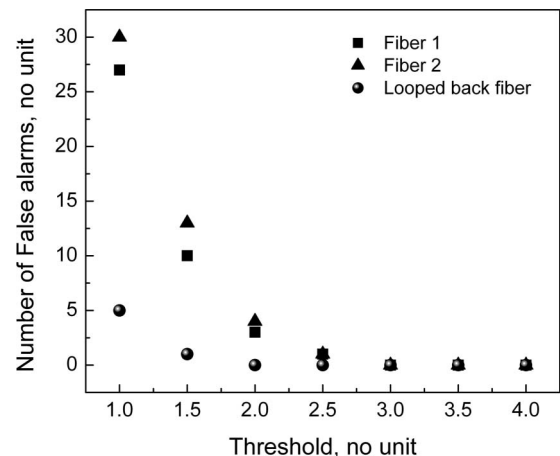


Fig. 8. Number of false alarm events registered as a function of threshold. A reduction in false alarms using the looped back mode is clearly seen.

at  $L$ , but also in the adjacent zones on either side. This may be due to the spreading of the leaking medium during percolation. When the leak begins, at 10,800 s, the percolating liquid reaches the fiber and heats it. Because both fibers sense temperature, a positive alarm for leakage is recorded after 10,860 s for  $2\sigma$  and at 10,890 s for  $4\sigma$  (Fig. 7). This time delay, 60 s for  $2\sigma$ , is the time taken by the leaking liquid to percolate to the fiber.

Figure 8 plots the number of false alarms events registered, as a function of *threshold* at room temperature. At  $1\sigma$ , the numbers of false alarms for fiber 1 and fiber 2 are 1033 and 1302, respectively. This corresponds to 11.97% and 15.1% of the total number of events. The number of false alarms with the looped back mode at the same threshold is 78. The ratio of false alarms with the looped back fiber mode to single fiber at  $1\sigma$  is 0.9%. The improvement in reliability can be clearly seen.

## 6. Conclusion

In this paper, a methodology to reduce the false alarm rate by using a looped back fiber mode has been demonstrated. The methodology proposed does not require any additional hardware, multiplexing, or multiple systems. The concept can be extended by introducing more segments of fiber passing over the same region and introducing suitable voting logic to improve reliability. Measurements at each of these zones are made with a single transition of the probing pulse along the length of the fiber. Thus, there will be no burden on measurement time by introducing additional measuring zones.

The authors thank the reviewers and the topical editor Catherine Towers for bringing lucidity to the paper.

## References

1. R. L. Tricker, *Optoelectronic and Fiber Optic Technology* (Newnes, 2002), pp. 23–28.
2. E. Udd, "Fiber optic smart structures," *Proc. IEEE* **84**, 60–76 (1996).
3. M. Bimpas, A. Amditis, and N. Uzunoglu, "Detection of water leaks in supply pipes using continuous wave sensor operating at 2.45 GHz," *J. Appl. Geophys.* **70**, 226–236 (2010).
4. D. S. Kupperman and T. N. Claytor, "Current practice and development efforts for leak detection in US reactor primary systems," in *Continuous Surveillance of Reactor Coolant Circuit Integrity* (Organisation for Economic Co-operation and Development/Nuclear Energy Agency, 1986), pp. 157–164.
5. A. Seibold, J. Bartonicek, and H. Kockelmann, "Operational monitoring in German nuclear power plants," *Nucl. Eng. Des.* **159**, 1–27 (1995).
6. K. Aoki, "Reactor coolant pressure boundary leak detection systems in Japanese PWR plants," *Nucl. Eng. Des.* **128**, 35–42 (1991).
7. A. MacLean, C. Moran, W. Johnston, B. Culshaw, D. Marsh, and P. Parker, "Detection of hydrocarbon fuel spills using a distributed fibre optic sensor," *Sens. Actuators A, Phys.* **109**, 60–67 (2003).
8. S.-C. Huang, W.-W. Lin, M.-T. Tsai, and M.-H. Chen, "Fiber optic in-line distributed sensor for detection and localization of the pipeline leaks," *Sens. Actuators A, Phys.* **135**, 570–579 (2007).
9. Z. Qu, H. Feng, Z. Zeng, J. Zhuge, and S. Jin, "A SVM-based pipeline leakage detection and pre-warning system," *Measurement* **43**, 513–519 (2010).
10. J. J. Smolen and A. Van der Speck, "Distributed temperature sensing—a DTS primer for oil & gas production," unclassified Shell report EP2003 (2003).
11. F. Jensen, E. Takada, M. Nakazawa, T. Takahashi, T. Kakuta, and S. Yamamoto, "Development of a distributed monitoring system for temperature and coolant leakage," in *Proceedings of the IAEA OECD/NEANSC Incore 96 Meeting* (Nuclear Energy Agency, 1996).
12. M. Nikles, B. Vogel, F. Briffod, S. Grosswig, F. Sauser, S. Luebbecke, A. Bals, and T. Pfeiffer, "Leakage detection using fiber optics distributed temperature monitoring," *Proc. SPIE* **5384**, 18–25 (2004).
13. M. Nikles, "Long-distance fiber optic sensing solutions for pipeline leakage intrusion and ground movement detection," *Proc. SPIE* **7316**, 731602 (2009).
14. D. Inaudi, R. Belli, and R. Walder, "Detection and localization of micro-leakages using distributed fiber optic sensing," in *7th International Pipeline Conference IPC2008* (ASME, 2008), paper IPC 2008-64280.
15. F. Tanimola and D. Hill, "Distributed fibre optic sensors for pipeline protection," *J. Natural Gas Sci. Eng.* **1**, 134–143 (2009).
16. J. Zhang, "Designing a cost effective and reliable pipeline leak detection system," presented at the Pipeline Reliability Conference, Houston, Texas, USA, 19–22 November 1996.
17. J. Bush, C. Davis, P. Davis, A. Cekorich, and F. McNair, "Buried fiber intrusion detection sensor with minima false alarm rates," *Proc. SPIE*, **3489**, 30–40 (1998).
18. J. A. Buck, *Fundamentals of Optical Fibers* (Wiley Interscience, 2004), pp 103–112.
19. C. Pandian, M. Kasinathan, S. Sosamma, C. Babu Rao, N. Murali, T. Jayakumar, and B. Raj, "One-dimensional temperature reconstruction for Raman distributed temperature sensor using path delay multiplexing," *J. Opt. Soc. Am. B* **26**, 2423–2426 (2009).
20. C. E. Stroud and J. K. Tannehill, Jr., "Applying built-in self-test to majority voting fault tolerant circuits," in *16th IEEE VLSI Test Symposium* (1998), pp. 303–308.
21. P. Swaminathan, "Design aspects of safety critical instrumentation of nuclear installations," *IJNEST* **1**, 254–263 (2005).
22. M. Höbel, J. Ricka, M. Wüthrich, and Th. Binkert, "High resolution distributed temperature sensing with the multiphoton-timing technique," *Appl. Opt.* **34**, 2955–2967 (1995).
23. P. di Vita and U. Rossi, "The backscattering technique: its field of applicability in fiber diagnostics and attenuation measurements," *Opt. Quantum Electron.* **12**, 17–22 (1980).
24. J. P. Dakin, D. J. Pratt, G. W. Bibby, and J. N. Ross, "Distributed optical fibre Raman temperature sensor using a semiconductor light source and detector," *Electron. Lett.* **21**, 569–570 (1985).